Boron nanowires for flexible electronics

Jifa Tian, Jinming Cai, Chao Hui, Chendong Zhang, Lihong Bao, Min Gao, Chengmin Shen, and Hongjun Gao[a)]
Institute of Physics, Chinese Academy of Sciences, Beijing 100190, People's Republic of China

(Received 9 June 2008; accepted 6 August 2008; published online 24 September 2008)

Flexible boron nanowires have been synthesized via thermoreduction in boron-oxygen compounds with magnesium. These as-prepared nanowires, which are structurally uniform and single crystalline, represent good semiconductor at high temperature. Tensile stress measurements demonstrate excellent mechanical property of boron nanowires as well as resistance to mechanical fracture even under a strain of 3%. Importantly, simultaneous electrical measurement reveals that the corresponding electrical conductance is very robust and remains constant under mechanical strain. Our results can be briefly explained by Mott's variable range hopping model. © *2008 American Institute of Physics*. [DOI: 10.1063/1.2976668]

Analogous to the revolutionary miniaturization in electronic industry initiated in 1950s, flexible electronics might also change the world in the future.[1] While recent rapid progress has been achieved in flexible technology,[2,3] one major technological challenge is to seek a suitable material that can retain excellent electrical performance even under large mechanical strain. Recently, significant efforts have been applied to two different types of flexible nanomaterials: inorganic semiconductors and organic conducting materials. The high-performance inorganic electronic materials such as silicon tend to fracture under 1% tensile strain. While single-walled carbon nanotubes have shown great promise for applications in flexible electronics, ill control of structural chirality makes them a big challenge for being useful in high-performance integrated circuits.[1,3]

Among well-known light elements such as B, C, and N, boron possesses many unique properties. Similarly to carbon and silicon, boron shows an obvious tendency to form covalent molecular compounds, but differs dramatically from carbon in having one less valence electron than the number of valence orbitals, a situation sometimes referred to as "electron deficiency."[4] Boron not only is the third lightest solid element with a low density of 2.340 g/cm^3 and a high melting point of 2300 °C, but also has a large bulk Young's modulus of 380–400 GPa and an extreme hardness close to diamond. These unique mechanical and electronic features make boron and its related compounds promising for future application in flexible technology. Particularly, recent theoretical work on boron and AlB_2 nanotubes[5,6] have stimulated significant experimental interest, in which the boron nanotubes were predicted to be metallic, independent of its chirality. So far, different techniques have been developed to fabricate one dimensional boron nanostructures. Amorphous boron nanowires were successfully fabricated by chemical vapor transport,[7] radio-frequency magnetron sputtering,[8,9] or laser ablation technique.[10] Ill-defined crystalline boron nanowires were directly synthesized by chemical vapor deposition reaction of diborane (B_2H_6) in Ar gas.[11] Tetragonal and rhombohedral boron nanostructures have been realized by laser ablation and thermal vapor transport process, respectively.[12–15] More recently, boron nanocones have been successfully synthesized in our group.[16] Nevertheless, due to the low productivity and poor quality of the boron nanowires, detailed characterization of their physical properties has been lacking.[11,17] Here, we reported a synthetic route for growth of boron nanowires and investigated their potential applications in flexible electronics.

Our work is based on a synthetic route to grow single crystalline boron nanowires on Si (111) through active metal (magnesium) thermal reduction in B/B_2O_3 in a H_2/Ar mixture gas at 1100 °C with Fe_3O_4 nanoparticles[18,19] as catalyst. Boron powder (99.9%), boron oxide (B_2O_3) powder (99.99%), and magnesium (99.99%) in a molar ratio of 10:1:3 were grounded together as precursors. A high temperature tube furnace was applied for synthesis with accurate control of temperature and gas flow rate. Detailed growth conditions of boron nanowires are as follows. At first, 100 SCCM (SCCM denotes cubic centimeter per minute at STP) H_2/Ar carrier gas was introduced after the system was pumped below 10 Pa. When the temperature of furnace center reached 400 °C at a rate of 200 °C/h, it was kept for 30 min to eliminate remaining oleic acid and oleylamine on the catalysts. Then, the flow rate of the carrier gas was decreased to 50 SCCM and the system pressure was maintained at $3-4\times10^3$ Pa. The system was then heated to 1100 °C at a rate of 200 °C/h without changing the system pressure. Boron nanowires were grown under this condition for 2 h. After that, the furnace was cooled down to room temperature, dark brown or black products were found on the surface of the substrate.

Morphologies of boron nanowires were examined by field-emission-type scanning electron microscope (SEM). Transmission electron microscopy (TEM) and high-resolution transmission electron microscopy (HRTEM) with electron energy loss spectrometer (EELS) were employed to perform the microanalysis of boron nanowires. In electrical measurements, the contact electrodes of device 1 deposited were fabricated by electron beam lithography (EBL) as follows. First, boron nanowires were placed on a SiO_2 insulating layer (500 nm thick) on Si (111) wafer. Then, four Ni/Au (20/130 nm) Ohmic contact electrodes were defined on a single boron nanowire with EBL and followed by thermal evaporation and lift-off processes. For comparison, four Pt

a)Author to whom correspondence should be addressed. Electronic mail: hjgao@aphy.iphy.ac.cn.

 © 2008 American Institute of Physics

Author complimentary copy. Redistribution subject to AIP license or copyright, see http://apl.aip.org/apl/copyright.jsp

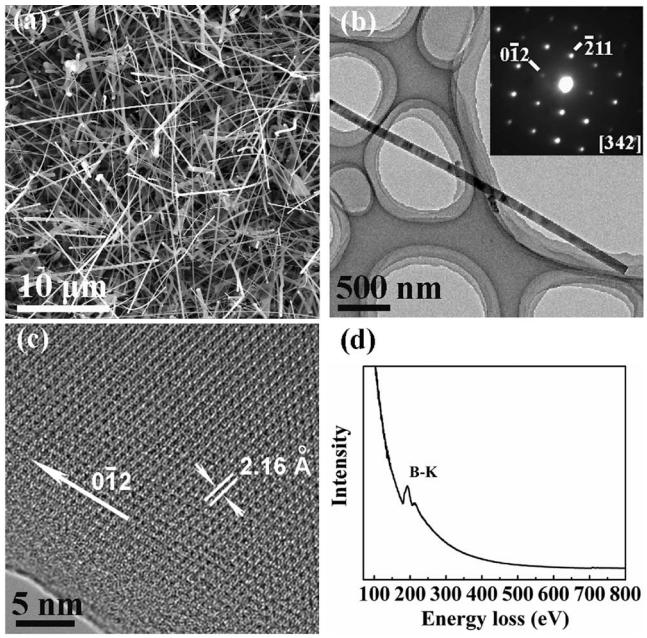

FIG. 1. (a) A typical SEM image of boron nanowires on Si (111) substrate. (b) TEM image of a single boron nanowire. The inset is the corresponding SAED pattern that can be indexed to β-rhombohedral boron. (c) HRTEM image of boron nanowire. The growth direction is along $[0\bar{1}2]$. (d) A typical EELS spectrum from an individual nanowire.

(100 nm) Ohmic contact electrodes on single boron nanowires were also directly fabricated by focused ion bean (FIB). Electrical transport flexibility measurements were conducted using four-probe scanning tunneling microscope (STM) system.[20,21]

Typical morphologies and microstructure of boron nanowires are shown in Fig. 1. These nanowires are about tens of micrometers long and 50–200 nm wide with random growth directions [Figs. 1(a) and 1(b)]. More detailed structure of nanowires can be further characterized by TEM and selected area electron diffraction (SAED), further revealing crystalline lattice fringes without observable defects [Figs. 1(b) and 1(c)]. The growth direction is along $[0\bar{1}2]$ and the measured lattice distance is about 2.16 Å, agreeing with $(\bar{2}03)$ lattice plane of β-rhombohedral boron. Figure 1(d) shows the typical EELS spectrum of the nanowire. The characteristic B *K*-edge at 188 eV is clearly visible and no other peaks can be distinguished.

Figure 2(a) shows current versus bias voltage (*I-V*) characteristics of single boron nanowire measured under different temperatures. All of the *I-V* curves are linear and symmetrical under a bias voltage of up to 4 V, and the conductance increases with the temperature. At 460 K the conductance can be improved by three orders of magnitude as compared with that of 120 K, indicating that boron nanowire is a good semiconductor above room temperature. The electrical conductivity of this device 1 is about 4.4×10^{-4} $(\Omega\ \mathrm{cm})^{-1}$ at

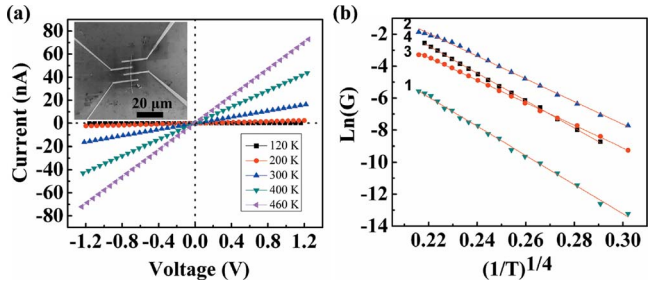

FIG. 2. (Color online) (a) The *I-V* characterization of boron nanowire. The inset gives the SEM image of device 1. (b) Temperature dependence of electrical conductivities of four different devices. The indexed numbers of each curve represent the corresponding devices.

room temperature, which is close to the value of bulk boron $(10^{-4}-10^{-7})$.[22,23] For comparison, device 2 was made by EBL but it was mended by FIB at the contacts between the boron nanowire and the electrodes. The conductivity of device 2 is 3.6×10^{-2} $(\Omega\ \mathrm{cm})^{-1}$, which is two orders higher than that of device 1. The same behavior was also observed in device 3 and 4, which were realized by FIB using Pt as the electrodes. Such conductivity enhancement can be attributed to the doping atoms (Ga and Pt) introduced in the FIB process.

Figure 2(b) gives linear relationships between $\mathrm{Ln}(G)$ and $(1/T)^{1/4}$ of these four devices. Here, G is the conductivity and T is the temperature. Such linear dependence can be understood by Mott's variable range hopping (VRH) model, assuming that the carrier transport occurs by thermal activation process between the localized states. According to Mott's law for the three-dimensional VRH, the conductivity G is expressed as

$$G = G_0 \exp\left\{-\left(\frac{T_0}{T}\right)^{1/4}\right\}, \tag{1}$$

$$T_0 = \frac{60}{\pi k_B l^3 N(E_F)}, \tag{2}$$

where l is the localization length of the carrier's wave function, $N(E_F)$ is the electron density of (localized) states at the Fermi level (E_F), k_B is the Boltzmann constant, and G_0 is a constant. The corresponding fit parameters T_0 of the temperature range are listed in Table I. Our data agree with this model well.

We further observed that the conductance of boron nanowires is very robust even under large strain. In this experiment one end of the boron nanowire was fixed by a Pt electrode fabricated by FIB [Figs. 3(a)–3(d)]. Also, one of the tips made of Au in the four-probe STM system was used as an electrode (in a two terminal configuration) and a manipulator [Figs. 3(a)–3(d)]. The electrical conductance measurement can be monitored during the process of bending. Both the Au and Pt electrodes have good Ohmic contacts with the

TABLE I. Model parameter T_0 of Mott's VRH model. The parameters for bulk samples of β-rhombohedral B (in Ref. 23) are also shown for comparison.

Samples	β-rhombohedral B (polycrystalline)	β-rhombohedral B (single crystal)	Device 1	Device 2	Device 3	Device 4
T_0 (K)	5.1×10^9	8.7×10^7	6.8×10^7	2.56×10^7	2.47×10^7	5.4×10^7

Author complimentary copy. Redistribution subject to AIP license or copyright, see http://apl.aip.org/apl/copyright.jsp

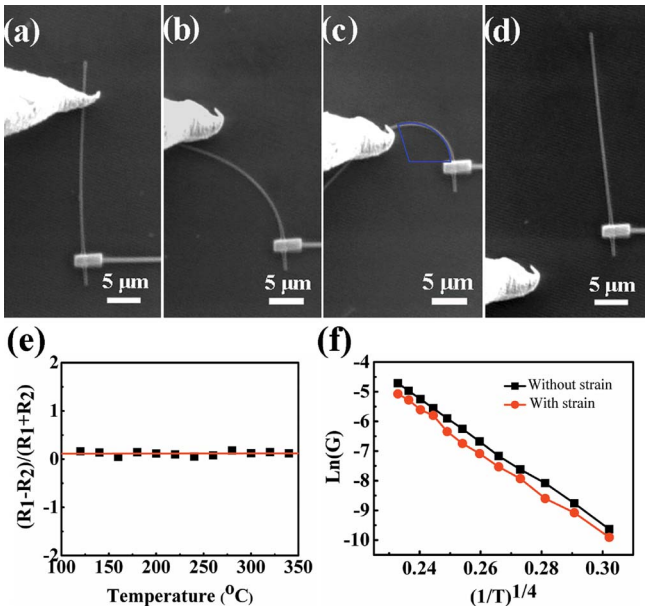

FIG. 3. (Color online) (a)–(d) SEM images showing mechanical bending process. (e) The relationship between $(R_1-R_2)/(R_1+R_2)$ and temperature T. (f) Temperature dependence of conductivities of nanowires with and without mechanical strain.

boron nanowire. The mechanical strain of nanowire experienced can be quantized as $\varepsilon=r/R$, where r and R represent the nanowire's radius and the radius of curvature, respectively. The nanowire remains intact even after 3% strain bending [Fig. 3(c)], which manifests excellent resilience as compared with single crystal bulk counterpart.[3] Importantly, the resistance of boron nanowire is very robust and remains almost unchanged while increasing the strain step by step. The resistivities measured under the situation of Figs. 3(a)–3(c) are 139.3, 143.8, and 142.4 Ω cm, respectively. The variation in resistivities might be due to different contact conditions during the electrode fabrication process. Figure 3(e) shows independence of $(R_1-R_2)/(R_1+R_2)$ on temperature T, where R_1 and R_2 are the resistances of boron nanowire without strain and with 3% strain, respectively. This independence of electrical conductance on mechanical strain can also be directly seen in Fig. 3(f). Our observed temperature dependent transport process of boron nanowire with strain also agrees well with Mott's VRH mechanism. Compared with the result of curve without strain (slope is −70.4), the slope under strain was almost the same (−70.31), which further suggests that strain on boron nanowires did not change its electron density of (localized) states at the Fermi level. Our results of robust electrical conductance of boron nanowires suggest that it might be an excellent candidate for flexible electric device.

In summary, we have developed a synthetic route for making high quality boron nanowires. The electrical transport of single boron nanowire shows room temperature conductivity of 4.4×10^{-4} $(\Omega\ \mathrm{cm})^{-1}$ and follows Mott's VRH mechanism. This electrical conductivity is very robust under mechanical strain of up to 3%. We believe that all our results together suggest that boron nanowires are promising nanoscale building blocks for flexible nanoelectronics.

The work is partially supported by the National 973 Program (Grant No. 2007CB935503), 863 Program (Grant No. 2007AA03Z305) and National Science Foundation of China (Grant Nos. 60571045 and U0734003).

[1] S. Hong and S. Myung, Nat. Nanotechnol. **2**, 207 (2007).
[2] Y. Sun, W. M. Choi, H. Jiang, Y. Y. Huang, and J. A. Rogers, Nat. Nanotechnol. **1**, 201 (2006).
[3] X. Lu and Y. Xia, Nat. Nanotechnol. **1**, 163 (2006).
[4] V. I. Matkovich, *Boron and Refractory Borides* (Springer, New York, 1977).
[5] A. Gindulyte, W. N. Lipscomb, and L. Massa, Inorg. Chem. **37**, 6544 (1998).
[6] I. Boustani, A. Quandt, E. Hernandez, and A. Rubio, J. Chem. Phys. **110**, 3176 (1999).
[7] Y. Y. Wu, B. Messer, and P. D. Yang, Adv. Mater. (Weinheim, Ger.) **13**, 1487 (2001).
[8] L. M. Cao, Z. Zhang, L. L. Sun, C. X. Gao, M. He, Y. Q. Wang, Y. C. Li, X. Y. Zhang, G. Li, J. Zhang, and W. K. Wang, Adv. Mater. (Weinheim, Ger.) **13**, 1701 (2001).
[9] L. M. Cao, K. Hahn, Y. Q. Wang, C. Scheu, Z. Zhang, C. X. Gao, Y. C. Li, X.Y. Zhang, L. L. Sun, W. K. Wang, and M. Ruhle, Adv. Mater. (Weinheim, Ger.) **14**, 1294 (2002).
[10] X. M. Meng, J. Q. Hu, Y. Jiang, C. S. Lee, and S. T. Lee, Chem. Phys. Lett. **370**, 825 (2003).
[11] C. J. Otten, O. R. Lourie, M. F. Yu, J. M. Cowley, M. J. Dyer, R. S. Ruoff, and W. E. Buhro, J. Am. Chem. Soc. **124**, 4564 (2002).
[12] Y. J. Zhang, H. Ago, M. Yumura, T. Komatsu, S. Ohshima, K. Uchida, and S. Iijima, Chem. Commun. (Cambridge) **2002**, 2086.
[13] S. H. Yun, A. Dibos, J. Z. Wu, and D. K. Kim, Appl. Phys. Lett. **84**, 2892 (2004).
[14] Z. K. Wang, Y. Shimizu, T. Sasaki, K. Kawaguchi, K. Kimura, and N. Koshizaki, Chem. Phys. Lett. **368**, 663 (2003).
[15] T. T. Xu, J. G. Zheng, N. Q. Wu, A. W. Nicholls, J. R. Roth, D. A. Dikin, and R. S. Ruoff, Nano Lett. **4**, 963 (2004).
[16] X. J. Wang, J. F. Tian, T. Z. Yang, L. H. Bao, C. Hui, F. Liu, C. M. Shen, C. Z. Gu, N. S. Xu, and H. J. Gao, Adv. Mater. (Weinheim, Ger.) **19**, 4480 (2007).
[17] D. W. Wang, J. G. Lu, C. J. Otten, and W. E. Buhro, Appl. Phys. Lett. **83**, 5280 (2003).
[18] T. Z. Yang, C. M. Shen, Z. A. Li, H. R. Zhang, C. W. Xiao, S. T. Chen, Z. C. Xu, D. X. Shi, J. Q. Li, and H. J. Gao, J. Phys. Chem. B **109**, 23233 (2005).
[19] F. Liu, P. J. Cao, H. R. Zhang, J. Q. Li, and H. J. Gao, Nanotechnology **15**, 949 (2004).
[20] X. Lin, X. B. He, J. L. Lu, L. Gao, Q. Huan, D. X. Shi, and H. J. Gao, Chin. Phys. **14**, 1536 (2005).
[21] X. Lin, X. B. He, T. Z. Yang, W. Guo, D. X. Shi, H. J. Gao, D. D. D. Ma, S. T. Lee, F. Liu, and X. C. Xie, Appl. Phys. Lett. **89**, 043103 (2006).
[22] *Landolt-Börnstein Numerical Data and Functional Relationships, New Series, Group III*, edited by K. H. Hellwege (Springer, Berlin, 1983), Vol. 17, Pt. E, p. 16.
[23] R. Schmechel, H. Werheit, V. Kueffel, and T. Lundstrom, *Proceedings of the 16th IEEE International Conference on Thermoelectrics*, 26–29 August 1997 (IEEE, New York), p. 219.

Author complimentary copy. Redistribution subject to AIP license or copyright, see http://apl.aip.org/apl/copyright.jsp